

DYNAMIC ANALYSIS OF A DISCRETE AMENSALISM MODEL WITH ALLEE EFFECT

Qimei Zhou¹, Yuming Chen^{1,†}, Shangming Chen¹
and Fengde Chen¹

Abstract This paper concerns with a discretization of a continuous-time amensalism model with Allee effect on the first species. Compared with the continuous analog, the discrete system has different and quite rich dynamical behavior. First, we obtain the existence of fixed points and their local stabilities. Then we confirm the occurrence of fold bifurcation and period doubling bifurcation by using the center manifold theorem and bifurcation theory. Followed is a hybrid control strategy to control the period-doubling bifurcation and stabilize unstable periodic orbits embedded in the complex attractor. Numerical simulations indicate that Allee effect is beneficial to the stability of the first species to a certain extent. Moreover, when the first species is affected by Allee effect, solutions can quickly approach the corresponding fixed point.

Keywords Amensalism model, Allee effect, fold bifurcation, period-doubling bifurcation, hybrid control strategy.

MSC(2010) 34C23, 34D20, 34H10, 92D25.

1. Introduction

In Nature, species are always interacting with each other. A lot of works have been done for predation, competition, and mutualism. However, amensalism has just got the attention of researchers in the last few decades. Amensalism is a biological interaction where one species causes harm to another organism without any cost or benefit to itself. There are two modes of amensalism, antibiosis and competition. An example of antibiosis amensalism is that in the African savannah, where large herbivores such as elephants inadvertently injure and even kill small ground-dwelling arthropods by trampling and compacting the soils and incurring no cost to themselves [20]. An example of competition amensalism is that grasshoppers significantly suppressed caterpillar feeding, growth rate, survival, reproductive effort and delayed metamorphosis in Tibetan alpine meadows. In contrast, the performance of grasshoppers was unaffected by caterpillars [27].

Based on the classic Lotka-Volterra model, Sun [24] firstly proposed the following

[†]The corresponding author.

¹School of Mathematics and Statistics, Fuzhou University, Fuzhou 350116, China

²Department of Mathematics, Wilfrid Laurier University, Waterloo, ON N2L 3C5 Canada

Email: 1324783421@qq.com(Q. Zhou), yuchen@wlu.ca(Y. Chen),
1070242634@qq.com(S. Chen), fdchen@263.net(F. Chen)

amensalism model of two species,

$$\begin{cases} \frac{dx}{dt} = r_1 x \left(\frac{k_1 - x - cy}{k_1} \right), \\ \frac{dy}{dt} = r_2 y \left(\frac{k_2 - y}{k_2} \right), \end{cases} \quad (1.1)$$

where $x(t)$ and $y(t)$ represent the densities of the first and second species at time t , respectively; r_1 and r_2 stand for the intrinsic growth rates of x and y , respectively; k_1 and k_2 are the environmental capacities of x and y , respectively; $c > 0$ reflects the impact exerted by the second species on the first species. Here y is harmful to x but x has no effect on y . Since then, the model has been modified by many researchers to incorporate other factors such as nonlinear functional responses [5, 15, 17], Allee effect [10, 25, 31], and refuge [14, 26, 28].

In 1931, Allee [1] observed that when the population density is too sparse or crowded, it will affect the reproduction rate of the population, which is not conducive to the growth of the species. When the population density is too low, individuals will face significant challenges in finding spouses and resisting natural enemies. This will lead to the decline of population birth rate and the increase of mortality. Such a phenomenon is called the Allee effect. In general, population models with Allee effect tend to exhibit very complex dynamical behavior because Allee effect may change the stability of equilibrium points to make a formerly stable system no longer stable. Recently, Guan and Chen [10] considered the Allee effect on the second species in an amensalism model with the Beddington-DeAngelis functional response. Their results show that the system with an Allee effect takes longer time to reach a stable steady-state solution than that without Allee effect. Wei *et al.* [25] found that the dynamic behaviors of an amensalism system become complicated by introducing weak Allee effect. Inspired by the above, Zhao and Du [31] proposed the following amensalism system with weak Allee effect on the first species,

$$\begin{cases} \frac{dx}{dt} = x \left(\frac{r_1 x}{m + x} - a_{11} x - a_{12} y \right), \\ \frac{dy}{dt} = y(r_2 - a_{22} y), \end{cases} \quad (1.2)$$

where all parameters r_1 , r_2 , a_{11} , a_{12} , a_{22} , and m are positive constants. The term $\frac{x}{m+x}$ denotes the weak Allee effect, where m describes the intensity of Allee effect on the first species. Their findings indicated that the dynamical properties of the amensalism model become complex when the first species is subject to the Allee effect. On the one hand, compared with the model without Allee effect, the number of equilibrium points of system (1.2) increases; On the other hand, when selecting coefficients α as a bifurcation parameter, authors proved the existence of saddle-node bifurcation.

As we know, data from biological samples are collected at discrete or specific times. Therefore, it is reasonable to assume that the use of discrete-time models is more realistic than continuous-time models. Moreover, existing studies have shown that discrete-time models can produce much richer dynamical behaviors than their continuous-time counterparts. Recently, Zhou *et al.* [33] systematically studied the discrete version of model (1.1). They found that the local stability property of the fixed points becomes complicated and the discrete version of model (1.1) would generate flip bifurcation at the only positive fixed point. Interestingly, many scholars

have explored the consequences and different ways of incorporating Allee effects into discrete-time population models. Bifurcation and stability are examined in detail in [4, 6, 8, 12, 13, 19, 21, 21, 23, 29, 30, 32]. For example, Yan *et al.* [29] proposed a discrete-time predator-prey model with linear functional response and Allee effect. It is found that the prey species with Allee effect would increase the extinction risk of both prey and predator. The bifurcations and chaos control of a discrete-time model with strong Allee effect on the prey are studied by Zhang and Zou [30]. They analyzed all possible codimension-two bifurcations at fixed points. Eskandari *et al.* [8] discussed a discrete-time predator-prey model with Allee effect on the prey population, whose results show that the model may generate various bifurcations such as transcritical, flip (period-doubling), and Neimark-Sacker bifurcations. However, not much has been done for the stability analysis of discrete amensalism systems subject to Allee effect.

Motivated by the above discussions, in this work we study the discretized version of the continuous model (1.2). We first nondimensionalize (1.2) by letting $\bar{x} = \frac{a_{11}x}{r_2}$, $\bar{y} = \frac{a_{22}y}{r_2}$, and $\bar{t} = r_2t$. After dropping the bars, system (1.2) becomes

$$\begin{cases} \frac{dx}{dt} = x \left(\frac{\alpha x}{m\gamma + x} - x - \beta y \right), \\ \frac{dy}{dt} = y(1 - y), \end{cases} \quad (1.3)$$

where $\alpha = \frac{r_1}{r_2}$, $\beta = \frac{a_{12}}{a_{22}}$, and $\gamma = \frac{a_{11}}{r_2}$. According to [2, 7], the piecewise constant argument method is a better choice for discretization of continuous models. This leads to the modification of system (1.3) as

$$\begin{cases} \frac{1}{x(t)} \frac{dx(t)}{dt} = \frac{\alpha x([t])}{m\gamma + x([t])} - x([t]) - \beta y([t]), \\ \frac{1}{y(t)} \frac{dy(t)}{dt} = 1 - y([t]), \end{cases} \quad (1.4)$$

where $[t]$ denotes the integer part of t . Then integrating (1.4) gives

$$\begin{cases} x(t) = x(n) \exp \left(\left[\frac{\alpha x(n)}{m\gamma + x(n)} - x(n) - \beta y(n) \right] (t - n) \right), \\ y(t) = y(n) \exp \left([1 - y(n)] (t - n) \right) \end{cases}$$

for $t \in [n, n + 1)$ and $n = 0, 1, 2, \dots$. Letting $t \rightarrow (n + 1)^-$ gives the discrete amensalism model to be studied,

$$\begin{cases} x_{n+1} = x_n \exp \left[\frac{\alpha x_n}{m\gamma + x_n} - x_n - \beta y_n \right], \\ y_{n+1} = y_n \exp[1 - y_n], \end{cases} \quad (1.5)$$

where we have denoted $x(n)$ and $y(n)$ respectively by x_n and y_n as usual. Clearly, the parameters α , β , and γ are all positive. Also from the point view of biology, we assume that the initial values (x_0, y_0) of system (1.5) are positive, that is, $x_0 > 0$ and $y_0 > 0$.

The aim of this paper is to understand the dynamical behavior of (1.5). We first investigate the existence and local stability of fixed points in Section 2. These results indicate possible occurrences of bifurcations. Then we analyze the fold bifurcation and period-doubling bifurcation in Section 3 and Section 4, respectively. Followed is a hybrid control method in Section 5 to stabilize the chaotic behavior due to period-doubling bifurcation. These theoretical findings are supported by numerical simulations in Section 6. The paper ends with a brief summary and comparison.

2. Stability analysis of system (1.5)

A fixed point (x, y) of (1.5) satisfies

$$x = x \exp\left(\frac{\alpha x}{m\gamma + x} - x - \beta y\right), \quad y = y \exp(1 - y). \quad (2.1)$$

Obviously, (1.5) always has the boundary fixed points $E_0(0, 0)$ and $E_1(0, 1)$. Moreover, if $\alpha > m\gamma$ then it also has a boundary fixed point $E_2(\alpha - m\gamma, 0)$. These are the possible boundary fixed points of (1.5). For possible positive fixed points, we must have $y = 1$. Substituting it into the first equation of (2.1), we see that x satisfies

$$x^2 + (\beta + m\gamma - \alpha)x + \beta m\gamma = 0. \quad (2.2)$$

Since we require $x > 0$, it is necessary that $\alpha > \beta + m\gamma$. Let Δ denote the discriminant of the quadratic in (2.2),

$$\Delta = \alpha^2 - 2(\beta + m\gamma)\alpha + (\beta - m\gamma)^2.$$

Then

$$\Delta \begin{cases} > 0 & \text{if } \alpha > \alpha_2 \stackrel{\text{def}}{=} \beta + m\gamma + 2\sqrt{\beta m\gamma}, \\ = 0 & \text{if } \alpha = \alpha_2, \\ < 0 & \text{if } \beta + m\gamma < \alpha < \alpha_2, \end{cases}$$

which implies that (2.2) has two positive roots $x_1^* = \frac{\alpha - \beta - m\gamma - \sqrt{\Delta}}{2}$ and $x_2^* = \frac{\alpha - \beta - m\gamma + \sqrt{\Delta}}{2}$ if $\alpha > \alpha_2$ while it has a unique positive root $x_3^* = \sqrt{\beta m\gamma}$ if $\alpha = \alpha_2$. The discussion is summarized in the following result.

Theorem 2.1. *The following statements on fixed points of (1.5) are true.*

- (i) *It only has the two boundary fixed points E_0 and E_1 if $0 < \alpha \leq m\gamma$.*
- (ii) *It has three boundary fixed points E_0, E_1, E_2 if $m\gamma < \alpha \leq \alpha_2$.*
- (iii) *It has three boundary fixed points E_0, E_1, E_2 , and a positive fixed point $E_3^* = (x_3^*, 1)$ if $\alpha = \alpha_2$.*
- (iv) *It has three boundary fixed points E_0, E_1, E_2 , and two positive fixed points $E_1^*(x_1^*, 1)$ and $E_2^*(x_2^*, 1)$ if $\alpha > \alpha_2$.*

Note that the Jacobian matrix of system (1.5) at a fixed point $E(x, y)$ is

$$J(E) = \begin{pmatrix} \left(1 - x + \frac{\alpha m\gamma x}{(m\gamma + x)^2}\right)M & -\beta x M \\ 0 & (1 - y)N \end{pmatrix} \quad (2.3)$$

where $M = \exp\left(\frac{\alpha x}{m\gamma + x} - x - \beta y\right)$ and $N = \exp(1 - y)$. Let λ_1 and λ_2 be the two eigenvalues of $J(E)$. Then E can be classified as follows [16].

Definition 2.1. The fixed point $E(x, y)$ of (1.5) is called

- (i) a sink if $|\lambda_1| < 1$ and $|\lambda_2| < 1$ and it is locally asymptotically stable;
- (ii) a source if $|\lambda_1| > 1$ and $|\lambda_2| > 1$, and it is unstable;
- (iii) a saddle if $\max\{|\lambda_1|, |\lambda_2|\} > 1$ and $\min\{|\lambda_1|, |\lambda_2|\} < 1$;
- (iv) non-hyperbolic if either $|\lambda_1| = 1$ or $|\lambda_2| = 1$.

Now we discuss the types of the fixed points of (1.5) obtained in Theorem 2.1. We start with the boundary fixed points.

Theorem 2.2. *The following statements on the boundary fixed points of (1.5) hold.*

- (i) $E_0(0, 0)$ is a non-hyperbolic point.
- (ii) $E_1(0, 1)$ is always a sink.
- (iii) When $\alpha > m\gamma$, the fixed point $E_2(\alpha - m\gamma, 0)$ is
 - (a) a saddle if $m\gamma < \alpha < \alpha^* \stackrel{\text{def}}{=} 1 + m\gamma + \sqrt{1 + 2m\gamma}$;
 - (b) a source (repeller) if $\alpha > \alpha^*$;
 - (c) non-hyperbolic if $\alpha = \alpha^*$.

Proof. It follows from (2.3) that

$$J(E_0) = \begin{pmatrix} 1 & 0 \\ 0 & e \end{pmatrix}, \quad J(E_1) = \begin{pmatrix} e^{-\beta} & 0 \\ 0 & 0 \end{pmatrix}, \quad J(E_2) = \begin{pmatrix} 1 - \frac{(\alpha - m\gamma)^2}{\alpha} & -\beta(\alpha - m\gamma) \\ 0 & e \end{pmatrix}.$$

Clearly, the eigenvalues of $J(E_0)$ are 1 and e (> 1), those of $J(E_1)$ are $e^{-\beta}$ ($\in (-1, 1)$) and 0; and those of $J(E_2)$ are $1 - \frac{(\alpha - m\gamma)^2}{\alpha}$ and e . Note that when $\alpha > m\gamma$,

$$1 - \frac{(\alpha - m\gamma)^2}{\alpha} \begin{cases} \in (-1, 1) & \text{if } m\gamma < \alpha < \alpha^*, \\ = -1 & \text{if } \alpha = \alpha^*, \\ < -1 & \text{if } \alpha > \alpha^*. \end{cases}$$

Thus the results immediately follow according to Definition 2.1. \square

Next we consider the positive fixed points of (1.5).

Theorem 2.3. *The following statements on positive fixed points of (1.5) are valid.*

- (i) Suppose that $\alpha = \alpha_2$. Then the unique positive fixed point $E_3^*(x_3^*, 1)$ of (1.5) is always non-hyperbolic.
- (ii) Suppose that $\alpha > \alpha_2$. Then $E_1^*(x_1^*, 1)$ is a saddle.
- (iii) Suppose that $\alpha > \alpha_2$. Then $E_2^*(x_2^*, 1)$ is
 - (a) a sink if $\alpha_2 < \alpha < \alpha^{**} \stackrel{\text{def}}{=} \frac{\beta^2 + \beta m\gamma + 2\beta + 2m\gamma + 2 + 2(\beta + 1)\sqrt{1 + (2 + \beta)m\gamma}}{2 + \beta}$;
 - (b) non-hyperbolic if $\alpha = \alpha^{**}$;
 - (c) a saddle if $\alpha > \alpha^{**}$.

Proof. The Jacobian matrix of system (1.5) at a positive fixed point $E_i^*(x_i^*, 1)$ ($i = 1, 2, 3$) is

$$J(E_i^*) = \begin{pmatrix} 1 - x_i^* + \frac{\alpha m \gamma x_i^*}{(m \gamma + x_i^*)^2} & -\beta x_i^* \\ 0 & 0 \end{pmatrix}, \tag{2.4}$$

whose eigenvalues are 0 and $1 - x_i^* + \frac{\alpha m \gamma x_i^*}{(m \gamma + x_i^*)^2}$. Noting $\frac{\alpha x_i^*}{m \gamma + x_i^*} = x_i^* + \beta$, we get

$$1 - x_i^* + \frac{\alpha m \gamma x_i^*}{(m \gamma + x_i^*)^2} = 1 - x_i^* + \frac{m \gamma}{m \gamma + x_i^*} (x_i^* + \beta) = 1 + \frac{\beta m \gamma - x_i^{*2}}{m \gamma + x_i^*}.$$

Since $x_1^* < x_3^* = \sqrt{\beta m \gamma} < x_2^*$, we have

$$1 - x_2^* + \frac{\alpha m \gamma x_2^*}{(m \gamma + x_2^*)^2} < 1 = 1 - x_3^* + \frac{\alpha m \gamma x_3^*}{(m \gamma + x_3^*)^2} < 1 - x_1^* + \frac{\alpha m \gamma x_1^*}{(m \gamma + x_1^*)^2},$$

which immediately gives (i) and (ii). For E_2^* , we further have

$$1 - x_2^* + \frac{\alpha m \gamma x_2^*}{(m \gamma + x_2^*)^2} = 1 + \frac{\beta m \gamma - x_2^{*2}}{m \gamma + x_2^*} \begin{cases} \in (-1, 1) & \text{if } x_2^* > 1 + \sqrt{1 + (2 + \beta)m\gamma}, \\ = -1 & \text{if } x_2^* = 1 + \sqrt{1 + (2 + \beta)m\gamma}, \\ < -1 & \text{if } x_2^* < 1 + \sqrt{1 + (2 + \beta)m\gamma}, \end{cases}$$

or equivalently by using the expression of x_2^* ,

$$1 - x_2^* + \frac{\alpha m \gamma x_2^*}{(m \gamma + x_2^*)^2} \begin{cases} \in (-1, 1) & \text{if } \alpha_2 < \alpha < \alpha^{**}, \\ = -1 & \text{if } \alpha = \alpha^{**}, \\ < -1 & \text{if } \alpha > \alpha^{**}. \end{cases}$$

Then (iii) follows and this completes the proof. □

Remark 2.1. Assume that $m = 0$ and $\alpha > \beta$. Then system (1.5) has only one positive fixed point $E^*(\alpha - \beta, 1)$. Especially, if $\beta < \alpha < \beta + 2$ holds, then $E^*(\alpha - \beta, 1)$ is asymptotically stable (see Fig. 1).

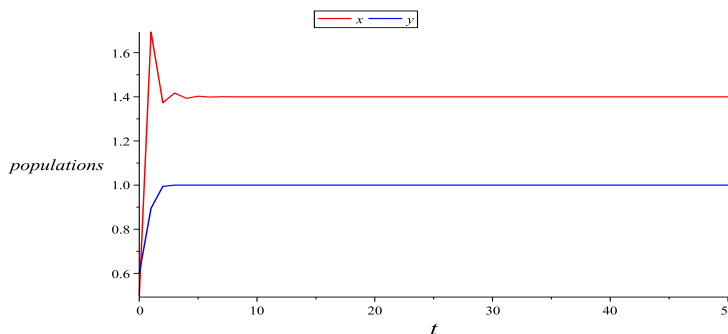


Figure 1. When $(\alpha, m, \beta) = (2.2, 0, 0.8)$, the unique positive fixed point $E^*(1.4, 1)$ of (1.5) is asymptotically stable. Here $(x_0, y_0) = (0.5, 0.6)$.

It is easy to see from the proofs of Theorem 2.2 and Theorem 2.3 that fold bifurcation may occur at E_3^* (the Jacobian matrix has an eigenvalue 1) and period-doubling bifurcation may occur at E_2 or E_2^* (the Jacobian matrix has an eigenvalue -1). Note that it can be inferred from (2.4) that model (1.5) does not show

Neimark-Sacker bifurcation and codimension-2 bifurcations by using Jury's criterion [9]. Hence we would use the bifurcation theory of normal forms and center manifold theorem [11, 22] to analyze all possible codimension-one bifurcations in the next two sections.

3. Fold bifurcation at E_3^*

Given β and $m\gamma$, when $\alpha = \alpha_2 = \beta + m\gamma + 2\sqrt{\beta m\gamma}$, there is a unique fixed point E_3^* and the eigenvalues of $J(E_3^*)$ are 1 and 0. Now, we investigate the fold bifurcation at the positive fixed point $E_3^*(x_3^*, 1)$ by treating α as the bifurcation parameter.

Let ζ be a small perturbation of α around α_2 , that is, $\alpha = \alpha_2 + \zeta$. Then system (1.5) is rewritten as

$$\begin{cases} x_{n+1} = x_n \exp\left(\frac{(\alpha_2 + \zeta)x_n}{m\gamma + x_n} - x_n - \beta y_n\right), \\ y_{n+1} = y_n \exp(1 - y_n). \end{cases} \quad (3.1)$$

First, we use the transform $U_n = x_n - x_3^*$, $V_n = y_n - 1$ to transform the fixed point E_3^* into the origin and system (3.1) into

$$\begin{cases} U_{n+1} = U_n + a_1\zeta + b_1V_n + w_{200}U_n^2 + w_{110}U_n\zeta + w_{101}U_nV_n \\ \quad + w_{020}\zeta^2 + w_{011}\zeta V_n + w_{002}V_n^2 + O\left(\left(|U_n| + |\zeta| + |V_n|\right)^3\right), \\ V_{n+1} = -\frac{1}{2}V_n^2 + O\left(\left(|U_n| + |\zeta| + |V_n|\right)^3\right), \end{cases} \quad (3.2)$$

where

$$\begin{aligned} a_1 &= \frac{\beta\sqrt{m\gamma}}{\sqrt{\beta} + \sqrt{m\gamma}}, & b_1 &= -\beta\sqrt{\beta m\gamma}, \\ w_{200} &= -\frac{\sqrt{\beta}}{\sqrt{\beta} + \sqrt{m\gamma}}, & w_{110} &= \frac{2\sqrt{\beta m\gamma} + \beta}{(\sqrt{\beta} + \sqrt{m\gamma})^2}, & w_{101} &= -\beta, \\ w_{020} &= \frac{\beta\sqrt{\beta m\gamma}}{2(\sqrt{\beta} + \sqrt{m\gamma})^2}, & w_{011} &= -\frac{\beta^2\sqrt{m\gamma}}{\sqrt{\beta} + \sqrt{m\gamma}}, & w_{002} &= \frac{\beta^2\sqrt{\beta m\gamma}}{2}. \end{aligned}$$

Next, with the non-singular change of variables

$$\begin{pmatrix} U_n \\ V_n \end{pmatrix} = \begin{pmatrix} a_1 & -b_1 \\ 0 & 1 \end{pmatrix} \begin{pmatrix} \tilde{x}_n \\ \tilde{y}_n \end{pmatrix},$$

system (3.2) becomes

$$\begin{cases} \tilde{x}_{n+1} = \tilde{x}_n + f_2(\tilde{x}_n, \zeta, \tilde{y}_n) + O\left(\left(|\tilde{x}_n| + |\zeta| + |\tilde{y}_n|\right)^3\right), \\ \tilde{y}_{n+1} = -\frac{1}{2}\tilde{y}_n^2 + O\left(\left(|\tilde{x}_n| + |\zeta| + |\tilde{y}_n|\right)^3\right), \end{cases} \quad (3.3)$$

where

$$f_2(\tilde{x}_n, \zeta, \tilde{y}_n) = \zeta + c_{200}\tilde{x}_n^2 + c_{110}\tilde{x}_n\zeta + c_{101}\tilde{x}_n\tilde{y}_n + c_{020}\zeta^2 + c_{011}\zeta\tilde{y}_n + c_{002}\tilde{y}_n^2$$

with

$$\begin{aligned} c_{200} &= -\frac{1}{\sqrt{\beta m \gamma}}, & c_{110} &= \frac{2}{\sqrt{\beta m \gamma}} - \frac{1}{\sqrt{\beta m \gamma + m \gamma}}, \\ c_{101} &= -\frac{\sqrt{\beta} + \sqrt{m \gamma}}{\sqrt{m \gamma}}, & c_{020} &= \frac{\sqrt{\beta}}{2(\sqrt{\beta} + \sqrt{m \gamma})}, \\ c_{011} &= -\beta, & c_{002} &= \frac{\sqrt{\beta}(\sqrt{\beta} + \sqrt{m \gamma})(1 + \beta)}{2}. \end{aligned}$$

Finally, express the center manifold $\mathcal{W}^c(0, 0)$ of (3.3) at the fixed point $(0, 0)$ in a small neighborhood of $\zeta = 0$ as

$$\mathcal{W}^c(0, 0) = \left\{ (\tilde{x}_n, \tilde{y}_n) : \tilde{y}_n = z_1 \tilde{x}_n^2 + z_2 \tilde{x}_n \zeta + z_3 \zeta^2 + O\left(\left(|\tilde{x}_n| + |\zeta|\right)^3\right) \right\}.$$

A simple calculation produces $z_1 = z_2 = z_3 = 0$. Thus the restricted system of (1.5) on the center manifold is

$$\tilde{x}_{n+1} = F_1(\tilde{x}_n) \stackrel{\text{def}}{=} \tilde{x}_n + \zeta + d_1 \tilde{x}_n^2 + d_2 \tilde{x}_n \zeta + d_3 \zeta^2 + O\left(\left(|\tilde{x}_n| + |\zeta|\right)^3\right),$$

where $d_1 = c_{200}a_1^2$, $d_2 = c_{110}a_1$, $d_3 = c_{020}$. Since

$$\begin{aligned} F_1(0, 0) &= 0, & \frac{\partial F_1}{\partial \tilde{x}}(0, 0) &= 1, & \frac{\partial F_1}{\partial \zeta}(0, 0) &= 1, \\ \frac{\partial^2 F_1}{\partial \tilde{x}^2}(0, 0) &= 2d_1 < 0, & \frac{\partial^2 F_1}{\partial \tilde{x} \partial \zeta}(0, 0) &= d_2 > 0, \end{aligned}$$

we have the following result.

Theorem 3.1. *System (1.5) undergoes a fold bifurcation at $E_3^*(x_3^*, 1)$ when $\alpha = \alpha_2$ holds. The fixed points $E_1^*(x_1^*, 1)$ and $E_2^*(x_2^*, 1)$ bifurcate from $E_3^*(x_3^*, 1)$ for $\alpha > \alpha_2$, coalesce at $E_3^*(x_3^*, 1)$ for $\alpha = \alpha_2$, and disappear for $\alpha < \alpha_2$.*

4. Period-doubling bifurcation

We start with period-doubling bifurcation at E_2 . From Theorem 2.2 (iii)(c), we know that if $\alpha = \alpha^* = 1 + m\gamma + \sqrt{1 + 2m\gamma}$ holds then E_2 exists and the eigenvalues of $J(E_2)$ are -1 and e . With α as the bifurcation parameter, it is easy to see that the central manifold of system (1.5) at $E_2(\alpha - m\gamma, 0)$ with $\alpha = \alpha^*$ is $y = 0$ and hence the restricted system of (1.5) on it is

$$x_{n+1} = f(x_n) = x_n \exp\left(\frac{\alpha x_n}{m\gamma + x_n} - x_n\right).$$

As $f'(x_n)|_{x_n=\alpha-m\gamma} = -1$, we know that $E_2(\alpha - m\gamma, 0)$ can experience period-doubling bifurcation when α is varied around α^* for given m and γ (see Fig. 3 (a)).

Now we discuss period-doubling bifurcation at $E_2^*(x_2^*, 1)$. Recall that $J(E_2^*)$ has an eigenvalue -1 when $\alpha = \alpha^{**} > \alpha_2$. Again α is chosen as the bifurcation parameter.

First, with $\alpha = \alpha^{**} + \xi$, system (1.5) is reexpressed as

$$\begin{cases} x_{n+1} = x_n \exp\left(\frac{(\alpha^{**} + \xi)x_n}{m\gamma + x_n} - x_n - \beta y_n\right), \\ y_{n+1} = y_n \exp(1 - y_n). \end{cases} \quad (4.1)$$

We use the transformation $u_n = x_n - x_2^*$ and $v_n = y_n - 1$ to transform the fixed point $E_2^*(x_2^*, 1)$ of (4.1) into the origin and (4.1) into

$$\begin{cases} u_{n+1} = a_{100}u_n + a_{010}v_n + a_{001}\xi + a_{200}u_n^2 + a_{110}u_nv_n + a_{101}u_n\xi \\ \quad + a_{020}v_n^2 + a_{011}v_n\xi + a_{002}\xi^2 + O\left(|u_n| + |v_n| + |\xi|\right)^3, \\ v_{n+1} = -\frac{1}{2}v_n^2 + O\left(|u_n| + |v_n| + |\xi|\right)^3, \end{cases} \quad (4.2)$$

where

$$\begin{aligned} a_{100} &= 1 - \frac{x_2^*[(x_2^* + m\gamma)^2 - \alpha^{**}m\gamma]}{(x_2^* + m\gamma)^2}, & a_{010} &= -\beta x_2^*, \\ a_{001} &= \frac{x_2^{*2}}{x_2^* + m\gamma}, & a_{002} &= \frac{x_2^{*3}}{2(x_2^* + m\gamma)^2}, \\ a_{200} &= \frac{x_2^*}{2} + \frac{\alpha^{**}m\gamma(1 - x_2^*)}{(x_2^* + m\gamma)^2} - 1 - \frac{\alpha^{**}x_2^*m\gamma[2(x_2^* + m\gamma) - \alpha^{**}m\gamma]}{(x_2^* + m\gamma)^4}, \\ a_{011} &= -\frac{\beta x_2^{*2}}{x_2^* + m\gamma}, & a_{110} &= \beta[x_2^* - 1 - \frac{\alpha^{**}x_2^*m\gamma}{(x_2^* + m\gamma)^2}], \\ a_{101} &= \frac{m\gamma x_2^*}{x_2^* + m\gamma} + \frac{m\gamma x_2^*[\alpha^{**}x_2^* + m\gamma + x_2^*]}{(x_2^* + m\gamma)^3}, & a_{020} &= \frac{\beta^2 x_2^*}{2}. \end{aligned}$$

Next, the non-singular change of variables

$$\begin{pmatrix} u_n \\ v_n \end{pmatrix} = \begin{pmatrix} a_{010} & a_{010} \\ -1 - a_{100} & -a_{100} \end{pmatrix} \begin{pmatrix} X_n \\ Y_n \end{pmatrix}$$

changes (4.2) into

$$\begin{cases} X_{n+1} = -X_n + F(u_n, v_n, \xi) + O\left(|u_n| + |v_n| + |\xi|\right)^3, \\ Y_{n+1} = G(u_n, v_n, \xi) + O\left(|u_n| + |v_n| + |\xi|\right)^3, \end{cases} \quad (4.3)$$

where

$$\begin{aligned} F(u_n, v_n, \xi) &= S_1\xi + S_2u_n^2 + S_3v_n^2 + S_4\xi^2 + S_5u_nv_n + S_6u_n\xi + S_7v_n\xi, \\ G(u_n, v_n, \xi) &= B_1\xi + B_2u_n^2 + B_3v_n^2 + B_4\xi^2 + B_5u_nv_n + B_6u_n\xi + B_7v_n\xi \end{aligned}$$

with

$$\begin{aligned} S_1 &= -\frac{a_{100}a_{001}}{a_{010}}, & S_2 &= -\frac{a_{100}a_{200}}{a_{010}}, & S_3 &= -\frac{a_{100}a_{020}}{a_{010}} + \frac{1}{2}, \\ S_4 &= -\frac{a_{100}a_{002}}{a_{010}}, & S_5 &= -\frac{a_{100}a_{110}}{a_{010}}, & S_6 &= -\frac{a_{100}a_{101}}{a_{010}}, \end{aligned}$$

$$\begin{aligned}
 S_7 &= -\frac{a_{100}a_{011}}{a_{010}}, & B_1 &= \frac{(1+a_{100})a_{001}}{a_{010}}, & B_2 &= \frac{(1+a_{100})a_{200}}{a_{010}}, \\
 B_3 &= \frac{(1+a_{100})a_{020}}{a_{010}} - \frac{1}{2}, & B_4 &= \frac{(1+a_{100})a_{002}}{a_{010}}, & B_5 &= \frac{(1+a_{100})a_{110}}{a_{010}}, \\
 B_6 &= \frac{(1+a_{100})a_{101}}{a_{010}}, & B_7 &= \frac{(1+a_{100})a_{011}}{a_{010}}.
 \end{aligned}$$

Let $W^c(0, 0)$ be the center manifold of (4.3) evaluated at $(0, 0)$ in a small neighborhood of $\xi = 0$. Then

$$W^c(0, 0) = \left\{ (X_n, Y_n) : Y_n = t_1\xi + t_2X_n^2 + t_3X_n\xi + t_4\xi^2 + O\left(\left(|X_n| + |\xi|\right)^3\right) \right\},$$

where

$$\begin{aligned}
 t_1 &= B_1, \\
 t_2 &= B_2a_{010}^2 + B_3(1+a_{100})^2 - B_5a_{010}(1+a_{100}), \\
 t_3 &= -2t_2S_1 - B_6a_{010} + B_7(1+a_{100}) - 2t_1B_2a_{010}^2 \\
 &\quad - 2t_1B_3a_{100}(1+a_{100}) + t_1B_5a_{100}a_{010}, \\
 t_4 &= t_1^2B_2a_{010}^2 + t_1^2B_3a_{100}^2 - t_1^2B_5a_{010}a_{100} + t_1B_6a_{010} \\
 &\quad - t_1B_7a_{100} - t_2S_1^2 + B_4 - t_3S_1.
 \end{aligned}$$

Therefore, the restricted difference equation of (4.3) on $W^c(0, 0)$ is given by

$$\begin{aligned}
 X_{n+1} = G^*(X_n) \stackrel{\text{def}}{=} & -X_n + h_0\xi + h_1X_n^2 + h_2X_n\xi + h_3\xi^2 + h_4X_n^2\xi \\
 & + h_5X_n\xi^2 + h_6X_n^3 + h_7\xi^3 + O\left(\left(|X_n| + |\xi|\right)^4\right),
 \end{aligned}$$

where

$$\begin{aligned}
 h_0 &= S_1, \\
 h_1 &= S_2a_{010}^2 + S_3(1+a_{100})^2 - S_5a_{010}(1+a_{100}), \\
 h_2 &= 2t_1S_2a_{010}^2 + 2t_1S_3a_{100}(1+a_{100}) - t_1S_5a_{100}a_{010} + S_6a_{010} - S_7(1+a_{100}), \\
 h_3 &= t_1^2S_2a_{010}^2 + t_1^2S_3a_{100}^2 + S_4 - t_1^2S_5a_{010}a_{100} + t_1S_6a_{010} - t_1S_7a_{100}, \\
 h_4 &= 2t_3S_2a_{010}^2 + 2t_1t_2S_2a_{010}^2 + 2t_3S_3(1+a_{100})a_{100} + 2t_1t_2S_3a_{100}^2 \\
 &\quad - t_3t_5a_{100}a_{010} - 2t_1t_2S_5a_{100}a_{010} + t_2S_6a_{010} - t_2S_7a_{100}, \\
 h_5 &= 2t_4S_2a_{010}^2 + 2t_1t_3S_2a_{010}^2 + 2t_4S_3(1+a_{100})a_{100} + 2t_1t_3S_3a_{100}^2 \\
 &\quad - t_4S_5a_{100}a_{010} - 2t_1t_3S_5a_{100}a_{010} + t_3S_6a_{010} - t_3S_7a_{100}, \\
 h_6 &= 2t_2S_2a_{010}^2 + 2t_2S_3(1+a_{100})a_{100} - t_2S_5a_{100}a_{010}, \\
 h_7 &= 2t_1t_4S_2a_{010}^2 + 2t_1t_4S_3a_{100}^2 - 2t_1t_4S_5a_{010}a_{100} + t_4t_6a_{010} - t_4S_7a_{100}.
 \end{aligned}$$

Define

$$\begin{aligned}
 \eta_1 &= \left(G_{X_n\xi}^* + \frac{1}{2}G_{\xi\xi}^*H_{X_nX_n}^* \right) \Big|_{(X_n,\xi)=(0,0)} = h_2 + h_0h_1, \\
 \eta_2 &= \left(\frac{1}{6}G_{X_nX_nX_n}^* + \left(\frac{1}{2}G_{X_nX_n}^*\right)^2 \right) \Big|_{(X_n,\xi)=(0,0)} = h_6 + h_1^2.
 \end{aligned}$$

Then we have the following result.

Theorem 4.1. *Given β , m , and γ , if $\eta_1 \neq 0$ and $\eta_2 \neq 0$, then system (1.5) undergoes period-doubling bifurcation at the fixed point $E_2^*(x_2^*, 1)$ when the parameter α varies in a small neighborhood of α^{**} . Moreover, if $\eta_2 > 0$ (resp., $\eta_2 < 0$) then the periodic-2 orbit is attracting (resp., repelling).*

5. Chaos control

Period-doubling bifurcation may lead to chaos. Chaos control and bifurcation theory is one of the most important and developed fields. In this section, we implement a hybrid control strategy of state feedback and parameter perturbation to control the period-doubling bifurcation at E_2^* [18].

To apply the hybrid control method, the corresponding controlled system is

$$\begin{cases} x_{n+1} = \varpi x_n \exp\left(\frac{\alpha x_n}{m\gamma + x_n} - x_n - \beta y_n\right) + (1 - \varpi)x_n, \\ y_{n+1} = \varpi y_n \exp(1 - y_n) + (1 - \varpi)y_n, \end{cases} \quad (5.1)$$

where $\varpi \in (0, 1)$ denotes the external control parameter. Note that (5.1) has the same structure of fixed points as (1.5). When $\alpha > \alpha_2$, the Jacobian matrix of the controlled system (5.1) evaluated at the positive fixed point $E_2^*(x_2^*, 1)$ is

$$J(E_2^*) = \begin{pmatrix} 1 + \left(\frac{\alpha m \gamma}{(m\gamma + x_2^*)^2} - 1\right) \varpi x_2^* & -\beta \varpi x_2^* \\ 0 & 1 - \varpi \end{pmatrix}.$$

The eigenvalues of $J(E_2^*)$ are $1 - \varpi \in (0, 1)$ and $1 + \left(\frac{\alpha m \gamma}{(m\gamma + x_2^*)^2} - 1\right) \varpi x_2^*$. We claim that $\frac{\alpha m \gamma}{(m\gamma + x_2^*)^2} - 1 < 0$. In fact,

$$\alpha m \gamma - (m\gamma + x_2^*)^2 = -\frac{(\alpha - \beta + m\gamma)\sqrt{\Delta}}{2} - \frac{H(\alpha)}{2},$$

where $H(\alpha) = \alpha^2 - 2(\beta + m\gamma)\alpha + (\beta - m\gamma)^2$. Note that H is strictly increasing on $[\beta + m\gamma, \infty)$. Then $H(\alpha) > H(\alpha_2) = 0$ for $\alpha > \alpha_2$. This shows $\alpha m \gamma - (m\gamma + x_2^*)^2 < 0$ and hence the claim is proved. Thus we have the following result.

Theorem 5.1. *Suppose that $\alpha > \alpha_2$. Then the positive fixed point $E_2^*(x_2^*, 1)$ of the controlled system (5.1) is locally asymptotically stable if and only if $\varpi x_2^* \left(1 - \frac{\alpha m \gamma}{(m\gamma + x_2^*)^2}\right) < 2$.*

We mention that chaos control at E_2 cannot be achieved.

6. Numerical examples

In this section, we present some numerical simulations to show the bifurcation diagrams and to demonstrate fascinating and complex dynamic behaviors of (1.5).

Example 6.1. In this example, we give the fold bifurcation diagram of system (1.5) at the fixed point $E_3^*(x_3^*, 1)$. Fix $m = 0.4$, $\gamma = 0.5$, and $\beta = 0.8$. Then $\alpha_2 = 1.8$ and there is a unique positive fixed point $E_3^*(0.4, 1)$. Fig. 2 gives the fold bifurcation diagram to support Theorem 3.1. We see from Fig. 2 that there are two positive fixed points if $\alpha > \alpha_2$, only one positive fixed point $E_3^*(0.4, 1)$ if $\alpha = \alpha_2$, and no positive fixed points if $\alpha < \alpha_2 = 1.8$.

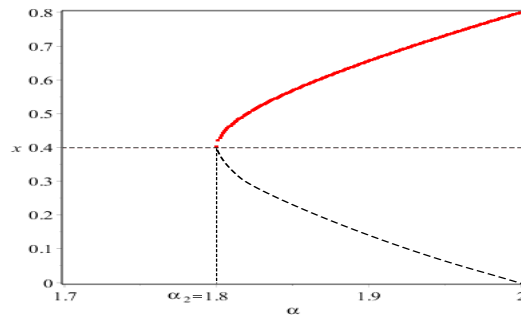


Figure 2. The fold bifurcation diagram of system (1.5) at the fixed point $E_3^*(x_3^*, 1)$ around the critical value $\alpha = \alpha_2 = 1.8$ when $m = 0.4, \beta = 0.8$ and $\gamma = 0.5$.

Example 6.2. In this example, we demonstrate the period-doubling bifurcation diagram of system (1.5) at $E_2^*(x_2^*, 1)$. We take $(\beta, m, \gamma) = (0.8, 0.5, 0.4)$ and $\alpha \in [2, 4.5]$. One can calculate that $\alpha^{**} \approx 3.32$. By Theorem 4.1, there is a period-doubling bifurcation at $E_2^*(2.25, 1)$ around $\alpha = \alpha^{**}$ (see Fig. 3(a) for the bifurcation diagram). The maximum Lyapunov exponent (MLE) is shown in Fig. 3(b). We

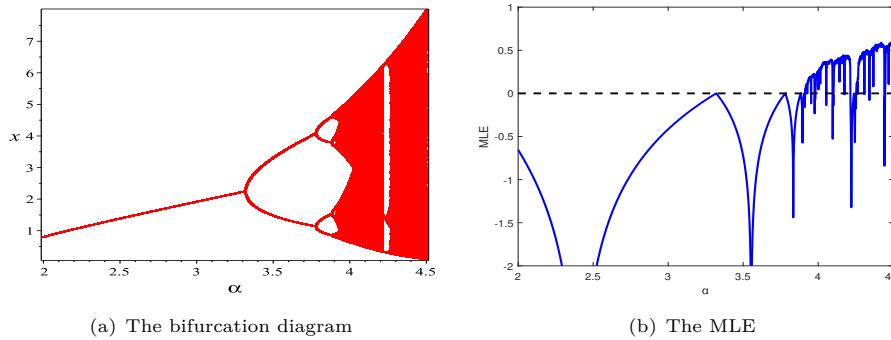


Figure 3. The period-doubling bifurcation diagram of (1.5) at $E_2^*(2.25, 1)$ with α as the bifurcation parameter. Here $(\beta, m, \gamma) = (0.8, 0.5, 0.4)$, which gives the critical value $\alpha = \alpha^{**} \approx 3.32$.

observe that the increase in the ratio of internal growth rate α makes system (1.5) chaotic starting from stable dynamics. However, being a planar system of ordinary differential equations, model (1.2) cannot possess chaotic dynamics.

For a more intuitive view of periodic orbits and chaotic sets, we plot the phase diagrams corresponding to each stage of Fig. 3 for six different values $\alpha = 3, 3.32, 3.5, 3.8, 3.9$ and 4.4 as examples in Fig. 4.

Example 6.3. To explore the impact of Allee effect on system (1.5), we can do the bifurcation analysis with m being a bifurcation parameter. To avoid repetition, we provide the simulations for period-doubling bifurcation at the positive fixed point $E_2^*(x_2^*, 1)$ by taking $(\gamma, \beta) = (0.4, 0.8)$. Fig. 5 (a) and (b) show the bifurcation diagrams for $\alpha = 3$ and 3.6 , respectively. On the one hand, the numerical result supports the claim in Example 6.2 that chaotic behavior occurs when α becomes larger. On the other hand, the larger the Allee effect constant m is, to a certain extent, the more beneficial to the stable coexistence of the population, but the level

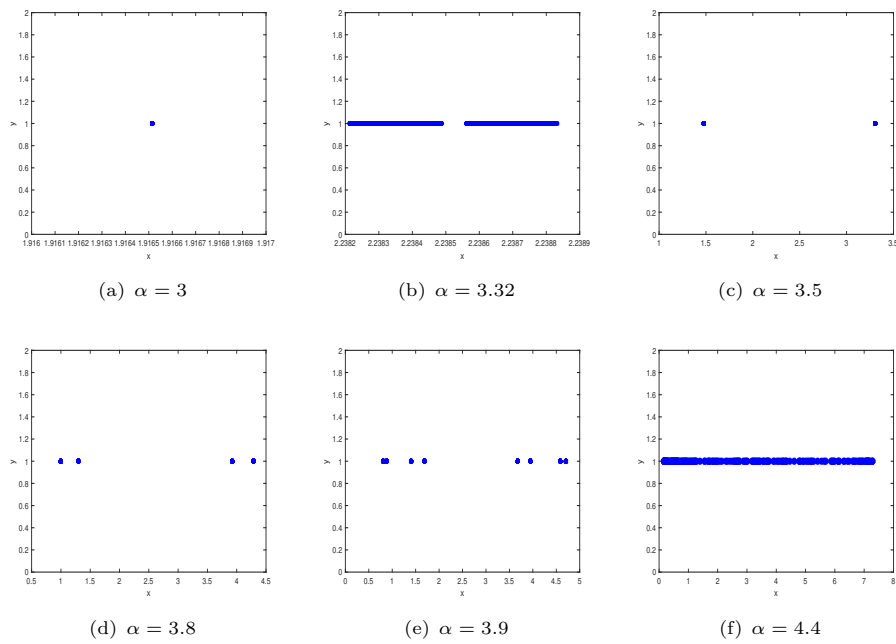


Figure 4. Phase portraits for various values of α corresponding to Fig. 3.

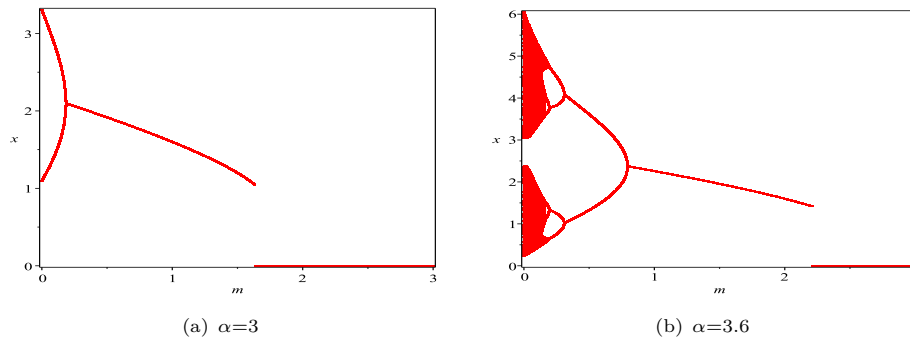


Figure 5. The bifurcation diagram with m being a bifurcation parameter

of the fixed point will be reduced. The concern is that too large Allee effect will force the first species to be extinct.

Example 6.4. In [3], Celik and Duman investigated the stability of discrete-time systems with and without Allee effect on the prey population. Through numerical simulations, they concluded that Allee effect can stabilize the prey population. In Example 6.3, we saw the stabilizing effect of Allee constant on the first species. We now further illustrate this by taking three different Allee constants ($m = 0, 0.5, 1.5$). The values of the other parameters for Fig. 6 (a) and (b) are the same as those for Fig. 5 (a) and (b), respectively. We further plot some trajectories in Fig. 7. Here $\gamma = 0.4$ and $\beta = 0.8$ for all figures, for Fig. 7(a), $\alpha = 3$ and $m = 0$, for Fig. 7(b), $\alpha = 3$ and $m = 1$, for Fig. 7(c), $\alpha = 3.6$ and $m = 0$, and for Fig. 7(d),

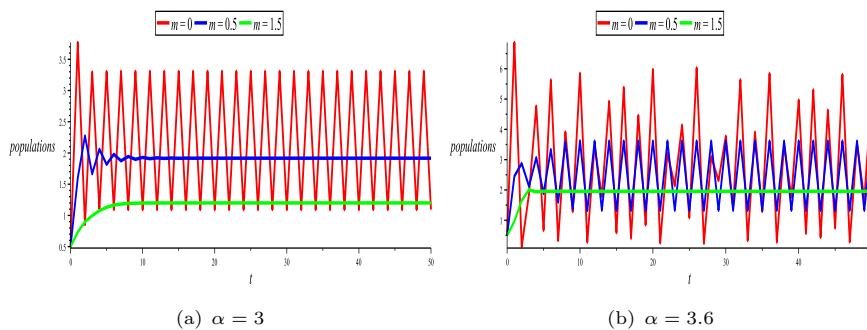


Figure 6. Time series of solutions of system (1.5) with different values of m .

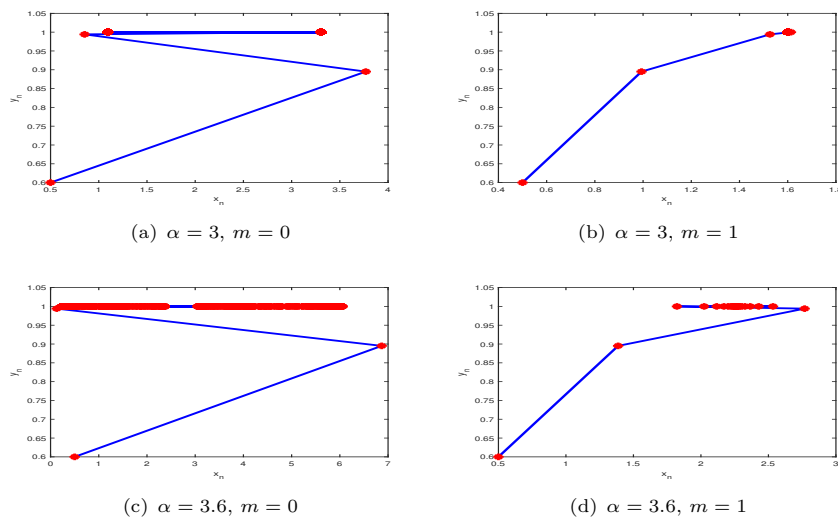


Figure 7. Trajectories of the densities of the first and second species with $(x_0, y_0) = (0.5, 0.6)$.

$\alpha = 3.6$ and $m = 1$. One can see from Fig. 7 (a) and (b) (or Fig. 7 (c) and (d)) that when the first species is subject to Allee effect, the corresponding solution spends short time to reach the positive fixed point. Moreover, we also observe that under Allee effect, the corresponding fixed point turns from unstable to stable.

Example 6.5. For chaos control, consider system (5.1) with $\alpha = 4.2$, $\beta = 0.8$, $m = 0.5$, and $\gamma = 0.4$. Then $x_2^* \approx 3.15$ and hence $\varpi x_2^* (1 - \frac{\alpha m \gamma}{(m \gamma + x_2^*)^2}) < 2$ if $0 < \varpi < 0.686$. Thus, according to Theorem 5.1, $(x_2^*, 1) = (3.15, 1)$ is locally asymptotically stable when $0 < \varpi < 0.686$. Moreover, $(x_2^*, 1) = (3.15, 1)$ is unstable when $\varpi \in (0.686, 1)$. Fig. 8 agrees with this, where $\varpi = 0.68$ in Fig. 8(a) and $\varpi = 0.69$ in Fig. 8(b). Note that the solution in Fig. 8(b) tends to a period-2 orbit.

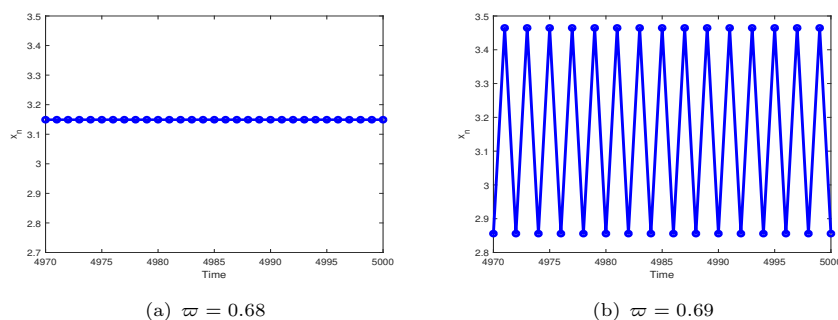


Figure 8. Time series of the first species for the controlled system (5.1) with different ϖ . Here $\alpha = 4.2$, $\beta = 0.8$, $m = 0.5$, $\gamma = 0.4$, and the initial condition is $(x_0, y_0) = (0.5, 0.6)$.

7. Summary and discussion

Though it is common, amensalism has not attracted enough attention of researchers as other interactions among species. In this paper, we studied a discrete amensalism model with Allee effect in the harmed species. This model is a discretization of a continuous-time one described by a system of two ordinary differential equations. The reason is that discrete models are more appropriate for species with non-overlapping generations and they have complicated dynamics compared with the continuous counterparts. The latter is also illustrated by this work. These findings suggest some strategies on species conservation and management by choosing appropriate intrinsic growth rates and Allee effect.

Compared with the discrete version of model (1.1) studied by Zhou *et al.* [33], system (1.5) has up to five fixed points and the dynamical properties become more complex. For example, a fold bifurcation occurs at the positive fixed point $E_3^*(x_3^*, 1)$ for system (1.5). Though the structure of fixed points of (1.5) is the same as that of the continuous counterpart (1.3), there are some differences in the local stabilities of fixed points. It is shown in [31] that $E_0(0, 0)$ may be a saddle-node or a non-hyperbolic saddle, $E_2(\alpha - m\gamma, 0)$ is a hyperbolic saddle, and $E_2^*(x_2^*, 1)$ is a hyperbolic stable node. Here we found that $E_0(0, 0)$ is always a non-hyperbolic point, and the types of $E_2(\alpha - m\gamma, 0)$ and $E_2^*(x_2^*, 1)$ depend on the value of α for given β , m , and γ (see Theorems 2.2 and 2.3). Furthermore, the proposed model has much rich dynamics including period-doubling bifurcation and even chaotic behavior.

It should also be pointed out that, based on Zhao and Du's work, we have demonstrated the stabilizing effect of Allee effect on the first species. In addition, the fixed point could be changed from chaos to stable or otherwise, and will spend short time to reach it when it is stable (see Example 6.3 and 6.4).

References

- [1] W. C. Allee, *Animal Aggregations: A Study in General Sociology*, University of Chicago Press, Chicago, 1931.
- [2] Z. AlSharawi, S. Pal, N. Pal, *et al.*, *A discrete-time model with non-monotonic functional response and strong Allee effect in prey*, *J. Difference Equ. Appl.*, 2020, 26(3), 404–431.

- [3] C. Celik and O. Duman, *Allee effect in a discrete-time predator-prey system*, Chaos Solitons Fractals, 2009, 40(4), 1956–1962.
- [4] P. Chakraborty, U. Ghosh and S. Sarkar, *Stability and bifurcation analysis of a discrete prey-predator model with square-root functional response and optimal harvesting*, J. Biol. Systems, 2020, 28(01), 91–110.
- [5] B. Chen, *Dynamic behaviors of a non-selective harvesting Lotka-Volterra amensalism model incorporating partial closure for the populations*, Adv. Difference Equ., 2018, 2018, Article ID: 111.
- [6] L. Cheng and H. Cao, *Bifurcation analysis of a discrete-time ratio-dependent predator-prey model with Allee effect*, Commun. Nonlinear Sci. Numer. Simul., 2016, 38, 288–302.
- [7] Q. Din, *Controlling chaos in a discrete-time prey-predator model with Allee effects*, Int. J. Dyn. Control, 2018, 6(2), 858–872.
- [8] Z. Eskandari, J. Alidousti, Z. Avazzadeh, et al., *Dynamics and bifurcations of a discrete-time prey-predator model with Allee effect on the prey population*, Ecol. Complex., 2021, 48, 100962.
- [9] S. Elaydi, *An Introduction to Difference Equation*, Springer-Verlag, 1996.
- [10] X. Guan and F. Chen, *Dynamical analysis of a two species amensalism model with Beddington-DeAngelis functional response and Allee effect on the second species*, Nonlinear Anal. Real World Appl., 2019, 48, 71–93.
- [11] J. Guckenheimer and P. Holmes, *Nonlinear Oscillations, Dynamical Systems, and Bifurcations of Vector Fields*, Springer Science & Business Media, 2013.
- [12] Z. Guo, H. Huo, Q. Ren, et al., *Bifurcation of a modified Leslie-Gower system with discrete and distributed delays*, J. Nonlinear Model. Anal., 2019, 1(1), 73–91.
- [13] S. Işık, *A study of stability and bifurcation analysis in discrete-time predator-prey system involving the Allee effect*, Int. J. Biomath., 2019, 12(01), 1950011.
- [14] C. Lei, *Dynamic behaviors of a stage structure amensalism system with a cover for the first species*, Adv. Difference Equ., 2018, 2018, Article ID: 272.
- [15] Q. Lin and X. Zhou, *On the existence of positive periodic solution of a amensalism model with Holling II functional response*, Commun. Math. Biol. Neurosci., 2017, 2017, Article ID: 3.
- [16] X. Liu and D. Xiao, *Complex dynamic behaviors of a discrete-time predator-prey system*, Chaos Solitons Fractals, 2007, 32, 80–94.
- [17] D. Luo and Q. Wang, *Global dynamics of a Holling-II amensalism system with nonlinear growth rate and Allee effect on the first species*, Internat. J. Bifur. Chaos Appl. Sci. Engrg., 2021, 31(03), 2150050.
- [18] X. Luo, G. Chen, B. Wang, et al., *Hybrid control of period-doubling bifurcation and chaos in discrete nonlinear dynamical systems*, Chaos Solitons Fractals, 2003, 18, 775–783.
- [19] R. Ma, Y. Bai and F. Wang, *Dynamical behavior analysis of a two-dimensional discrete predator-prey model with prey refuge and fear factor*, J. Appl. Anal. Comput., 2020, 10(4), 1683–1697.

- [20] D. L. Ogada, M. E. Gadd, R. S. Ostfeld, et al., *Impacts of large herbivorous mammals on bird diversity and abundance in an African savanna*, *Oecologia*, 2018, 156, 387–397.
- [21] S. S. Rana, *Bifurcations and chaos control in a discrete-time predator-prey system of Leslie type*, *J. Appl. Anal. Comput.*, 2019, 9(1), 31–44.
- [22] C. Robinson, *Dynamical Systems: Stability, Symbolic Dynamics and Chaos*, CRC Press, 1998.
- [23] Q. Su and F. Chen, *The influence of partial closure for the populations to a non-selective harvesting Lotka-Volterra discrete amensalism model*, *Adv. Difference Equ.*, 2019, 2019, Article ID: 281.
- [24] G. Sun, *Qualitative analysis on two populations amensalism model*, *Jiamusi University (Natural Science Edition)*, 2003, 21(3), 283–286.
- [25] Z. Wei, Y. Xia and T. Zhang, *Stability and bifurcation analysis of an amensalism model with weak Allee effect*, *Qual. Theory Dyn. Syst.*, 2020, 19(1), 1–15.
- [26] R. Wu, L. Zhao and Q. Lin, *Stability analysis of a two species amensalism model with Holling II functional response and a cover for the first species*, *J. Nonlinear Funct. Anal.*, 2016, 2016, Article ID: 46.
- [27] X. Xi, J. N. Griffin and S. Sun, *Grasshoppers amensalistically suppress caterpillar performance and enhance plant biomass in an alpine meadow*, *Oikos*, 2013, 122(7), 1049–1057.
- [28] X. Xie, F. Chen and M. He, *Dynamic behaviors of two species amensalism model with a cover for the first species*, *J. Math. Comput. Sci.*, 2016, 16, 395–401.
- [29] J. Yan, C. Li, X. Chen, et al., *Dynamic complexities in 2-dimensional discrete-time predator-prey systems with Allee effect in the prey*, *Discrete Dyn. Nat. Soc.*, 2016, 2016, Article ID: 4275372.
- [30] L. Zhang and L. Zou, *Bifurcations and control in a discrete predator-prey model with strong Allee effect*, *Internat. J. Bifur. Chaos Appl. Sci. Engrg.*, 2018, 28(05), 1850062.
- [31] M. Zhao and Y. Du, *Stability and bifurcation analysis of an amensalism system with Allee effect*, *Adv. Difference Equ.*, 2020, 2020, Article ID: 341.
- [32] M. Zhao, C. Li and J. Wang, *Complex dynamic behaviors of a discrete-time predator-prey system*, *J. Appl. Anal. Comput.*, 2017, 7(2), 478–500.
- [33] Q. Zhou, F. Chen and S. Lin, *Complex dynamics analysis of a discrete amensalism system with a cover for the first species*, *Axioms*, 2022, 11(8), 365.